"The Effects of Artesunate and Paclitaxel on Human Prostate Cancer Cell Lines"

by

Juan Pablo Fabian-Garcia

A Thesis submitted to the Graduate Faculty of

Elizabeth City State University in partial fulfillment of the

requirements for the Degree of Master of Science

Elizabeth City, North Carolina

2022

APPROVED BY

Dolapo A. Adedeji
Dolapo A. Adedeji (May 2, 2022 14:39 EDT)

Dr. Dolapo Adedeji, Chair of Thesis Committee

Hirendra Banerjee (May 2, 2022 16:24 EDT)

Dr. Hirendra Banerjee, Committee Member

Jeffrey M Rousch
Jeffrey M Rousch (May 2, 2022 17:42 EDT)

Dr. Jeffrey Rousch, Committee Member

Lloyd Mitchell PhD MPH

Dr. Lloyd Mitchell, PhD, MPH, Outside Examiner

ABSTRACT

In the present study, the combination of artesunate (ART) and paclitaxel (PTX) in two human prostate cancer (PCa) cell lines (PC-3 and LNCaP) was evaluated to investigate the effects on proliferation and apoptosis of PCa cells. The present study explored whether their effects were associated with reactive oxygen species (ROS). Half maximal inhibitory concentration (IC50) values were obtained for ART mM (2.126μM) and (0.05μM) PTX for LNCaP cells and for ART (25.1μM) and (3.98 μM) PTX μM for PC-3 cells at 72 and 120 h. Ratio combination were assessed by MTT assay using IC50 values at (1:1,1:2, 2:1) to evaluate ratio with least cell viability revealed LNCaP was ART1:PTX1 and PC-3 was ART2:PTX1. Annexin V and propidium iodide staining was used to investigate apoptosis by flow cytometry. The apoptotic mechanisms of ART + PTX in PCa were investigated by detecting activities of apoptosis, caspase-3/7, and intracellular ROS accumulation. ART + PTX induced PCa apoptosis, ROS accumulation, caspase 3/7 activity. Taken together, these results indicated that ART + PTX suppressed PCa cell proliferation in a dose- and time-dependent manner.

DEDICATION

I would like to dedicate this thesis in honor of my family especially my grandmother Merenciana, and close friends.

ACKNOWLEDGEMENTS

Thank you to my committee members Dr. Dolapo Adedeji, Dr. Hirendranath Banerjee, Dr. Jeffrey Rousch, and Dr. Lloyd Mitchell for their time, patience, and guidance throughout this process. The Office of Graduate Education for allowing me the opportunity to expand my educational horizon through the NOYCE program, the Historically Black Colleges and Universities (HBCUs) Masters Degree Program Grant for financial support of laboratory materials and donation of supplies from Dr. Banerjee. Thanks to my family, friends, peers for supporting me during the past two years of graduate school. In addition, I would like to acknowledge ECSU staff who helped during the graduate application process.

TABLE OF CONTENTS

LIST OF TABLES

LIST OF FIGURES

CHAPTER I

INTRODUCTION

General Cancer Information

In a normal physiological function, human cells grow and multiply through cell division to form new cells when needed. These new cells take the place of aged or damaged cells. When the cell division process is disrupted, abnormal or damaged cells grow and multiply uncontrollably to form tumors. Tumors are lumps of tissue that are classified as cancerous or benign. Cancerous tumors can start anywhere in the human body and have the potential to invade nearby tissues and travel to distant places in the body to form new tumors by a process called metastasis. Many cancers form solid tumors with the exception of a few such as leukemias which form in the blood. Benign tumors do not spread or invade nearby tissues. Unlike cancerous tumors, benign tumors usually do not grow back when removed (NIH, 2021). Cancer is considered a genetic disease that is caused by the change in DNA sequence that controls cell function to grow and divide. These genetic changes can occur due to errors as cell divides, damage to DNA caused by harmful substances that are introduced by the environment directly or indirectly, and by genetic inheritance. There are more than 100 types of cancers that are classified based on organ or tissue in which they form. Cancers can further be described by the type of cell that they form such as epithelial or squamous cells (NIH, 2021). General treatments for various cancers involve surgery, radiation, androgen deprivation therapy (ADT), chemotherapy, or a combination.

Prostate Cancer Formation

Prostate cancer is categorized as adenocarcinoma, defined by the abnormal development from the gland cells. In normal prostate functions, the prostate is the size of a walnut. The gland is located around the urethra at the base of the penis. The size of the prostate may change with age, in general cases it becomes much larger as men become elderly. It functions to produce about one-third of the fluid present in semen. This fluid aids in nourishing and maintaining a high pH for sperm survival (Leslie, 2021). The initial cellular characteristic of prostate cancer is mutations in the cells of the prostate gland that cause it to grow at accelerated rates. Recently,

there have been reported about 5,000 somatic mutations in prostate growth (Habib et al.,2021). The abnormal growth of cells spread to surrounding prostate tissue forming a tumor. This growth can stay in the prostate or continue to spread to nearby organs, in a process known as metastatic prostate cancer. The most common areas of which metastatic prostate cancer spreads are the bones and lymph nodes (Leslie, 2021).

Influences of Prostate Cancer

The cause of prostate cancer continues to be unclear although inflammation is found to be the generalization that leads to cancer. Inflammation is a key driver of prostate cancer metastasis and therapeutic resistance. Chronic inflammation has been identified as a major cause of approximately 20% of human cancer cases. Environmental exposure to bacterial, viral infections, dietary habits, hormonal influences, physical injury, exposure to mutagenic agents, and genetic variation predispose the prostate gland to inflammation. An inflammatory response is coordinated with an elevated expression of inflammatory cytokines. Chronic inflammation in the prostate can alter the tumor microenvironment suitable for cancer progression, proliferation, cell survival, metastasis spread and resistance to therapeutic agents. Inflammation in prostate progression can be detected in histology exams in which lesions containing activated inflammatory immune cells infiltrate with the peripheral zone of the prostate (Archer, Dogra & Kyprianou, 2020).

Tumor Microenvironment (TME) in Prostate Cancer

The tumor microenvironment of tissue is examined to understand tumor progression. It is comprised of proliferation tumor cells, blood vessels, infiltration inflammatory cells. This unique environment is created in the process of tumor progression with its host. The tumor influences molecular and cellular events that take place in surrounding tissues (Greten et al. 2019). Prostate cancer cells produce several inflammatory factors, which modify the tumor microenvironment that contribute to tumor cell growth, survival, invasion and progression. Prostate cancer cells and surrounding prostate stroma cells express high levels of inflammatory cytokines that promote tumor proliferation and survival. One of the major inflammatory signaling pathways is elicited

by the inflammatory NF-kB signaling pathway which is constitutively activated primary by cytokine TNF-alpha. This process aids in resistance to apoptosis by inducing expression of anti-apoptotic proteins such as Bcl-xL. Inflammatory cytokines play a role in enabling different stages in metastasis (Archer, Dogra & Kyprianou, 2020).

Epithelial-Mesenchymal Transition in Prostate Cancer

Epithelial-mesenchymal transition (EMT) is a biological process that allows immotile epithelial cells to convert into mesenchymal cells. This process plays a crucial role in tissue remodeling and development of tissue (Lai et al. 2020). This process can be recapitulated in cancer. During the phenotype transition of cancer, cells respond to intrinsic genetic and molecular alterations, or extrinsic microenvironment stimuli (Di et al. 2019). The EMT process leads to the detachment of tumor cells from the non-cellular portion of the tissue that contains material produced and secreted by surrounding cells referred to as the extracellular matrix (ECM). As the cells undergo EMT, they start to lose their cell-to-cell adhesions, and eventually detach from the ECM. In normal cell physiology, the cells are detached and go through the process of anoikis. This form of cell death is due to the absence of connection between the cells and ECM. In tumor cells, a resistance is developed to anoikis and allows cells to migrate freely in bodily fluid circulation, leading to metastasis. This leads to the development of prostate cancer therapeutic resistance to hormone treatment known as metastatic castration-resistant prostate cancer (mCRPC), and cancer patient mortality (Archer, Dogra & Kyprianou, 2020).

Statistics of Prostate Cancer

Every year, 20.7 out of 100,000 men die of prostate cancer and 11.11 % of men will be diagnosed with prostate cancer at some point (SEER,2019). Due to the growth and aging of the global population, it was estimated the global epidemiology of prostate cancer is increasing by approximately 1.7 million new cases per year and about 499,000 mortalities are expected by 2030 (Habib et al.,2021). The Food and Drug Administration (FDA) is constantly seeking prospective anticancer agents to be approved for various cancers. In drug discovery, out of every 5,000-10,000 candidates only 5% are chosen to be considered an oncology lead compound that

will ultimately be approved to enter Phase 1 clinical trial, these rates support the need for alternative efforts for drug discovery. Various registered drugs that have already been tested for safety and drug formulation may hold promise to rapid clinical trials for different indication than its original (Zhe et al.2016).

Artesunate

Artesunate (ART) is primarily an antimalarial drug used since 1973 for malaria caused by *Plasmodium falciparum* and cerebral malaria, although it has been shown to have some cytotoxic properties. In the 1990's, Artemisinin was first reported to have anticancer effects by *in vitro* and *in vivo* studies in a variety of tumor cells such as leukemia, colorectal cancer, melanoma, breast and prostate cancer, among others. This can make a promising repurposed agent for the treatment of prostate cancer. New insight brought by growing evidence showed that Artesunate are expected to be a new class of antitumor drug of wide spectrum (Zhe et al.2016).

Artesunate is isolated and extracted from dried leaves and buds of the Wormwood plant (*Artemisia annua L)* produced in southwest China. It is considered a semi-synthetic derivative, water soluble, sesquiterpene lactone compound that contains an endoperoxide radical without any nitrogen atoms in its structure. The main active anticancer sites of ART are the same as the antimalarial sites. All derivates focus on keeping the peroxide bridge and modification of other portions of compound (Zhe et al.2016). The ART derivatives target cell membranes as the principal target sites. They have not only been shown to induce apoptosis but play a role in cell swelling. The cytomembrane is destroyed in the process and the membrane permeability is altered which results in death of cells.

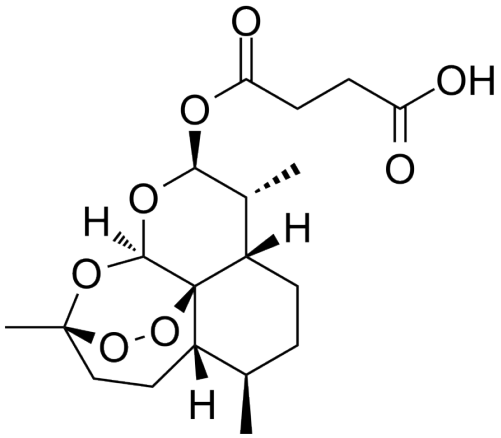

Fig. 1: Structure of Artesunate (ART)

Ovarian cancer cell lines demonstrated a strong induction of reactive oxygen species (ROS) and reduced proliferation when treated with ART. This caused damage to membranes, autophagy and apoptosis, including inhibiting angiogenesis of cancer cells. Additionally, cell cycle arrest is caused by the change of expression and activity in several regulatory enzymes. (Greenshields et al., 2017) In Ishikawa endometrial cancer cells, ART has induced G1 cell cycle arrest and downregulated cyclin-dependent kinase 4 gene expression which is seen to play a role in cancer progression (Yin et al. 2020).

Paclitaxel

Paclitaxel (PXT) is a taxane-class drug used for the treatment of prostate cancer. It is derived from the bark of the Pacific Yew Tree (*Taxus brevifolia).*Although registered and approved as a cancer therapy drug by FDA for the treatment of prostate cancer, it is limited due to the amount of serious side effects and recent occurring drug resistance. PXT's mechanism of action is to induce cell cycle arrest and apoptosis in most cancer cells. It works by binding and stabilizing the β-tubulin microtubule polymer interfering with the microtubule assembly of mitosis and prolonged activation in the G2/M phase of the cell cycle (Zhe et al.2016). Microtubules are characterized as hollow tubes formed through the heterodimerization of alpha and beta tubulin that results in polar protofilaments. Microtubules aid in functions for structural integrity,

transportation, migration, and are the main component that drives the growth and shrinking of size of mitotic spindles (Bumbaca et al., 2018).

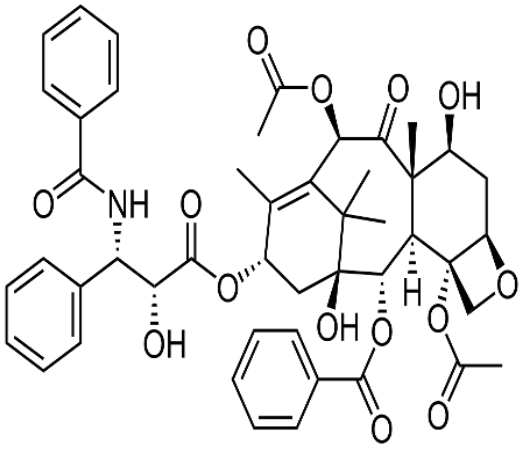

Fig. 2: Structure of Paclitaxel (PTX)

Some cancers may demonstrate resistance to paclitaxel through various mechanisms such as mutations of caspases in prostate carcinoma PC-3 cells. Due to paclitaxel cancer resistance literature supports the use of adjuvant treatment. The enhancement of paclitaxel-induced apoptosis through the use of adjuvant treatments has been shown for various cancers. Artesunate in combination with Paclitaxel could provide insight for apoptosis enhancement through similar mechanisms and reverse paclitaxel resistance through expression of proapoptotic proteins. ROS activity can potentiate the effect of paclitaxel thus increasing apoptosis rate in cell cycle arrest G0/G1 (Datta et al.,2019).

Purpose of Statement

Human prostate cancer (PCa) is increasing by approximately 1.7 million new cases per year worldwide with about 499,000 mortalities expected by 2030. This is due, in part, to the increases and aging of the global population (Habib et al.,2021). Current treatments for PCa, such as androgen deprivation therapy (ADT), surgical castration, and radiation therapy, can be effective, but there is a proportion of patients undergoing these treatments that relapse within a median of 2-3 years (Wadosky et al,2016). Paclitaxel (PXT), a taxane-class drug, induces G2/M phase cell cycle arrest and apoptosis, but prostate cancers may demonstrate some resistance to paclitaxel.. As such, the enhancement of PXT-induced apoptosis through adjuvant treatments are investigated in this work. Artesunate (ART) is an antimalaria drug that has shown anticancer effects and is being repurposed for cancer treatment. ART has demonstrated reactive oxygen species activity (ROS) activity following apoptosis via increase Bax mediated intrinsic in various studies. Artesunate in combination with Paclitaxel could provide insight for apoptosis enhancement through similar mechanisms and may reverse paclitaxel resistance. The specific aims of this proposed work are to assess the cytotoxicity properties of ART, PX, and ART+PXT in combination to determine the concentration at which 50% of prostate cancer cells die (IC50) and to assess the ROS and caspase 3/7 activity on various prostate cancer cell lines. Cell morphology based on cell membrane changes of prostate cell lines due to ART, PXT, ART+PXT combined exposure will also be assessed. To future elucidate mechanism, the Bax protein concentrations would be detected using western blot in prostate cancer cell lines exposed to ART, PXT and ART and PXT combined.

CHAPTER II
REVIEW OF LITERATURE

Prostate Cancer Cell Lines

PC-3 (androgen-independent) and LNCaP (androgen-dependent) prostate cancer cell lines have been extensively used as models to study prostate cancer progression to develop therapeutic agents. PC-3 is a prostatic adenocarcinoma that is metastatic to bone through seminal vesicles, whereas LNCaP is an adenocarcinoma that is metastasized to the left supraclavicular lymph node through lymph nodes lesions near the prostate (Dozmorov et al.,2009). In PC-3, there is no expression of androgen or prostate sensitive antigen (PSA), compared to LNCaP that expresses both. PC-3 represents castration resistant tumors that are usually aggressive compared to LNCaP. LNCaP represent androgen-dependent tumors that consists of the majority of clinical cases (Tai et al.,2011). Androgen receptor (AR) plays an important role in prostate carcinogenesis. In mouse knock out studies, during prostate development, stromal AR induced and promoted epithelial cell growth. Furthermore, during prostate carcinogenesis and progression, the stromal cells begin to lose AR expression as early as the stage of high-grade prostatic intraepithelial neoplasia. AR is a crucial mediator for anti-prostate cancer. (Archer, Dogra & Kyprianou, 2020).

Ferritin is a protein that stores and releases iron, which can be a prime target for ROS activity caused by chemotherapy. High ferritin levels were positively associated with increased serum prostate-specific antigen (PSA) levels and prostate cancer risk. Prostate tissue ferritin levels are significantly higher in prostate cancer patients compared to benign prostatic hyperplasia (BPH) controls. (Wang et al.,2017) In another study serum levels of selenium, zinc, copper, manganese, and iron in prostate cancer in patients, found that there is a decreased levels of Se, Zn, Mn, and increased Cu and Fe levels in different prostate cancers stages (Saleh et al.,2020)

Artesunate: ROS Mechanism

Artesunate has not been fully elucidated, although the C-radical hypothesis has become widely accepted. Toxic-free radicals such as hydroxyl radicals and superoxide ions are generated by the endoperoxide bridge moiety reacting with ferrous atom to produce reactive oxygen species (ROS) (Zhe et al.2016). ROS are correlated to induction of apoptosis and oxidative DNA damage. During the process tumor cells are killed or attenuated by ROS activity. Tumor cells are more susceptible to damage due to the lack of antioxidant enzymes. Tumor cells have high expression of transferrin receptor, which are more susceptible to ART and its derivates to stimulate cytotoxicity. ROS activity is considered to be a universal mechanism of anticancer drugs. The major organelles that are injured by artesunate induces oxidative stress are the mitochondrion, endoplasmic reticulum, and digestive vacuole (Pang et al.2016).

Artesunate: Cell Cycle Arrest

Artesunate has been seen to cause cell cycle arrest at different phases of interphase. In ovarian cancer cell lines, ROS-dependent cell arrest occurred in G2/M, while ROS-independent cell cycle arrest has occurred in G1 phase depending on concentration of ART (Greenshields et al.,2016). Cell cycle arrest has been shown to be a mechanism of both ART and PXT. Previous research indicates that ART induces cycle arrest in the G2/M phase by upregulating the expression of the Beclin1, which is an initiator of autophagy. Artesunate may interfere with genes that regulate mitotic spindle checkpoint in the G2/M phase such as Bub3, Mad3, and Mad2 (Zhe et al.2016).

Artesunate: Apoptosis

Artesunate induced apoptosis in various tumor cells including glioblastoma, T Leukemia, neuroblastoma, breast, embryonal rhabdomyosarcoma and lung cancers, and could demonstrate ROS-dependent apoptosis in prostate cancer. ART derivates have demonstrated proapoptotic activity by mitochondrial outer membrane permeabilization, an intrinsic pathway that is influenced by the release of cytochrome 3 and overexpression of Bax, by increase Bax/Bcl-2 ratio and activating caspase -3 and caspase-9 found in various cancers (Yang et al., 2020). Caspase 3, an executioner caspase will destroy cellular structures such as poly (ADP-ribose)

polymerase, an enzyme involved in DNA repair, causing cell death. Artesunate has been shown to induce ROS dependent apoptosis via Bax-mediated intrinsic apoptosis in human cancer cells

lines (Huh-7 and H3B) (Maz et al.,2021). Art dose-dependently suppressed tumor growth, inhibited cell viability, enhanced apoptosis, decreased AR expression, and AR receptor inhibition.

Paclitaxel: ROS Mechanism

Recently, some studies suggested that paclitaxel has direct effects on mitochondrial to induce mitochondrial permeability transition (MPT) and ROS generation. This mechanism is an effective chemotherapeutical approach that can selectively induce apoptosis of cancer cells. It is likely that PTX could bind to mitochondrial tubulin and thus resulting in the opening of mitochondrial permeability transition pore, and ultimately triggering the ROS release from mitochondria. Compared to nonproliferation cells, proliferation cancer cells have a higher level of free tubulin, and therefore, paclitaxel is relatively more selective for cancer cells and induces cancer cells to generate ROS (Iang et al.,2018).

Paclitaxel: Apoptosis

According to Ren (2019), treatment of CHMm cells with PTX resulted in a dose dependent decrease in the levels of anti-apoptotic proteins Bcl-2 and a simultaneous increase in pro-apoptotic protein Bax. The alteration is known to be responsible for the concomitant execution phase of apoptosis, including the disruption of mitochondrial membrane potential, increased release of cytochrome-c into cytoplasm and cleave of caspase 3 protein. Regulation of intrinsic apoptosis by Bcl-2 family proteins occur through ROS production and is followed by reduction in the MMP level, which stimulates mitochondria to release proapoptotic molecules and results in activation of caspase-9 and −3 (Ren et al., 2019). The results of the present study demonstrated that levels of ROS and MDA were elevated and reduced levels of SOD. These results indicated that paclitaxel induced alterations in expression of apoptosis-associated proteins and generation of ROS. However, it remains to be elucidated whether mitochondria-dependent apoptosis induced by paclitaxel is mediated by ROS; the mechanism in which paclitaxel

selectively induced apoptosis of CHMm cells has been defined but requires further investigation. Based on the results of the present study, treatment with paclitaxel induced cell apoptosis which may be mediated by downregulation of Bcl-2 and upregulation of Bax and is likely associated with the inhibition of the PI3K/AKT signaling and activation of MAPK signaling pathways (Ren et al., 2019).

Paclitaxel Resistance

One of the major reasons behind PTX resistance is the overexpression of drug efflux pumps, like MRP1 and MDR1. The Multidrug Resistance (MDR) family of efflux transporters is known to be heavily involved in resistance to various forms of chemotherapy. Increased phosphate glycoprotein (P-gp) expression, certain genetic variants of P-gp, as well as ABCC4 expression have also been linked to increased docetaxel resistance in prostate cancer. The clinical utility of P-gp inhibitors has not been effective and can potentially be toxic at their required doses for the treatment. In addition to this, mutation in beta tubulin have been associated with resistance to PTX, change in tubulin isoforms (beta III overexpression) (Bumbaca et al.,2018).

CHAPTER III

MATERIALS AND METHODS

Cell Viability Study

Prostate cancer cell lines (PC-3 and LNCaP) were purchased form the American Type Culture Collection (ATCC, Manassas, VA). LNCaP clone FGC (ATCC CRL-1740) and PC3 (ATCC CRL-1435) were cultured and maintained in Corning 75 cm canted neck flasks with Roswell Park Memorial Institute (RPMI)1640 medium containing fetal bovine serum (10%), penicillin-streptomycin (1%), sodium pyruvate (1%), glutamine and non-essential amino acids (1%). The cells were placed in a humidified environment at 37°C, supplied with 5% CO_2. The cell lines' media were replaced with fresh medium every 2-3 days, or variable depending on growth rate and rate of confluency for the flask. LNCaP and PC3 cell lines were harvested upon 70-80% confluency, by using 7 mL of trypsin EDTA (without sodium bicarbonate) after removing all growth medium. The flask was returned into the humidified environment for 10-15 min. The trypsin-cell solution was centrifuged for 6 min at 2.5 RPM The cell pellets were resuspended in 1 mL of medium. The cell suspension (1 mL) was aliquoted into a flask containing 10-12 mL of fresh medium for cell subculturing. In the process of cryopreservation, cell pellets were suspended in 5% DMSO and stored in cryopreservation vials at -80°C. LNCaP and PC3 were then seeded into 96-well plates at a density of $1x10^4$ cells/well in RPMI 1640 complete medium. Cells were given 24 h to attach to the flasks. Artesunate 100 mM stock solution was made by dissolving 0.1492 g artesunate in 10 mL of dimethyl sulfoxide (DMSO). Paclitaxel 1 mM stock solution was made by dissolving 0.0088 g paclitaxel in 5 mL of DMSO. Artesunate and paclitaxel were further diluted with RPMI medium to achieve desired concentrations used to treat cells. The RPMI medium in 96-well plates were aspirated and replaced with 200 µl of artesunate and paclitaxel at concentrations:1 mM, 0.1 mM, 0.01 mM, 0.001 mM 0.1 µM, 0.001 µM, 0.0001 µM. Experiments in which cells were treated with various concentration of artesunate and paclitaxel were performed in triplicate for each concentration. Treatments were conducted in 96 well plates with the addition of 200 µl of cells and treatments. In addition, the negative control contained wells of cells with the required density, and positive control row

contained cells within the density with 200 µl of 0.001% DMSO used to control for DMSO drug vehicle. (Hinton, Adedeji, & Payne,2017)

After 72 and 120 h exposure to treatments, viability of the cells was determined quantitatively by addition of the reducing agent 3-[4,5-dimethylthiazol-2-yl]-2,5-diphenyltetrazolium bromide (MTT). The yellow tetrazolium salt (MTT) is reduced by metabolically active cells by dehydrogenase enzyme, to generate reducing equivalents such as NADH and NADPH. The MTS tetrazolium compound is bio reduced by cells into a colored formazan product that is soluble in tissue culture medium. This conversion is also accomplished by metabolically active cells by dehydrogenase enzyme, to generate reducing equivalents such as NADH and NADPH. (Hinton, Adedeji, &Payne,2017). Twenty microliters of MTT were added to each well and plates returned to incubator at 37°C for 4 h until purple precipitate was visible under the microscope. The media was carefully aspirated and 200 µl of DMSO reagent was added to each well to dissolve the formazon crystals formed the reaction Plates were stored in dark a designated area without light overnight. Following an overnight incubation period, optical density was determined using the MultiSkan FT spectrophotometer set at 570 nm (ThermoFisher, USA). Cell viability was determined by comparing the optical density of treated versus the control cells. The inhibition rate of cell proliferation was calculated by the following formula:

$$\text{Growth inhibition} = \frac{OD_{Control} - OD_{Treated}}{OD_{Control}} x\ 100$$

The cytotoxicity effect of drugs on cancer cells were expressed in EC_{50} (the drug concentration reducing the absorbance of treated cells by 50 with respect to untreated cells). Using EC_{50} values, a combination study of 200 µl of ART+PTX at various ratios (2:1, 1:2, 1:1) were tested for their impacts on cell viability by MTT assay. The experiments were performed in triplicates for each concentration. In addition, the negative control contained wells of cells with the required density, and positive control contained cells within the density with 200 µl of 0.001% DMSO that were tested in parallel.

TACS® Annexin V-FITC Apoptosis Assay

The number of apoptotic cells were measured using TACS® Annexin V-FITC Apoptosis Detection Kit (Cat#4839-01-K). PC-3 and LNCaP cells were seeded at a concentration of 1 x10^5 cells/well overnight in a Corning Cellbind 6 well plate. Cell lines were treated with ART, PTX and ART:PTX based on the ratio with lower viability percentage. TACS® Annexin V conjugate with fluorescein isotheiocyanate (FITC) (USA R&D system, Minneapolis, MN) were added and incubated at 37°C for 15 min followed by addition of a binding buffer. Cells were washed with phosphate-buffered saline (PBS). The cells were analyzed for apoptosis and morphology based on cell membrane changes and fluorescence intensity using the flow cytometer at 494 nm and emission at 519 nm (Guava easyCyte single loader, USA) (Arbab et al., 2012).

Reactive oxygen species (ROS) detection

The production of intracellular of reactive oxygen species (ROS) generation was detected using 2'-7'-dichlorofluorescin diacetate (DCFH-DA)(Catalog# D6883) (EMD Millipore Corp, USA). This reagent can passively enter the cell membrane and react with the ROS to form fluorescent dichlorofluorescin (DCF) and the fluorescent intensity was measured. PC-3 and LNCaP cells were seeded at a concentration of 1 x10^5 cells/well overnight in a Corning Cellbind 6 well plate. After cell lines (PC-3 and LNCaP) were exposed to ART, PXT and ART:PXT ratios, 6 well plates were washed with Dulbecco's phosphate-buffered saline and then incubated in 10 μM of DCFH-DA at 37°C for 30 min. Fluorescence was then determined at 485 nm excitation and 520 nm emission using aflow cytometer (Guava easyCyte single loader, USA).

CellEvent™ Caspase 3/7 assay

LNCaP were seeded at 1x10^5 cell/well in a Corning Cellbind 6 well plate and treated with ART, PTX and ART:PXT ratio concentration for 72 h. Then, caspase activity was determined according to the CellEvent ™ Caspase- 3/7 Green Flow Cytometry Assay Kit (Catalog# C10427) (Invitrogen, USA) manufacturer's protocol. Equal volumes of 1 mL samples contained 1 μL of the CellEvent Caspase- 3/7 green detection reagent was added and incubated at room temperature for 30 min at 37°C following the addition of 1 μL of 1 mM SYTOX™ AADvanced™ dead stain cell solution

(Catalog# C10427). The presence of active caspases from apoptotic cells will leave the synthetic tetrapeptide (DEVD) with nucleic acid binding dye in the reagent. During apoptosis, caspase-3 and caspase-7 proteins are activated and are able to cleave the caspase 3/7 recognition sequence encoded in the DEVD peptide. Cleavage of the recognition sequence and binding of DNA by the reagent labels apoptotic cells with a bright, fluorogenic signal. The intensity was analyzed for LNCaP cancer cell lines at 488 nm excitation using a flow cytometer (Guava easyCyte single loader, USA)

CHAPTER IV

RESULTS

Cell Viability Study with ART and PTX

The LNCaP and PC3 prostate cancer cell lines were cultured and counted using the trypan blue assay assessed by Countess 3 FL Automated Cell Counter (Thermo Fisher Scientific, USA) to seed at an appropriate quantity of cells. The cell lines were treated with Artesunate and Paclitaxel compounds at concentrations of 1000 µM, 100 µM, 10 µM, 1 µM, 0.1µM, 0.01µM, 0.001µM. The exposure time was 72 hours (3 days) and 120 (5 days) to determine the IC_{50} values using MTT/MTS cell proliferation assays. The MTT assay was used in the analysis of detecting cell death. The two graphs were used to compare cytotoxic effects of at the specified time constraints. Results showed that there was not a distinct difference in cell death between the blank and control variables. Figures 3, demonstrates the IC_{50} values of Artesunate and Paclitaxel in PC-3 cell lines are 25.1µM and 3.98µM at 120 hours. Figures 4, demonstrates the IC_{50} values of Artesunate and Paclitaxel in LNCaP cell lines are 2.126µM and 0.05µM at 72 hours.

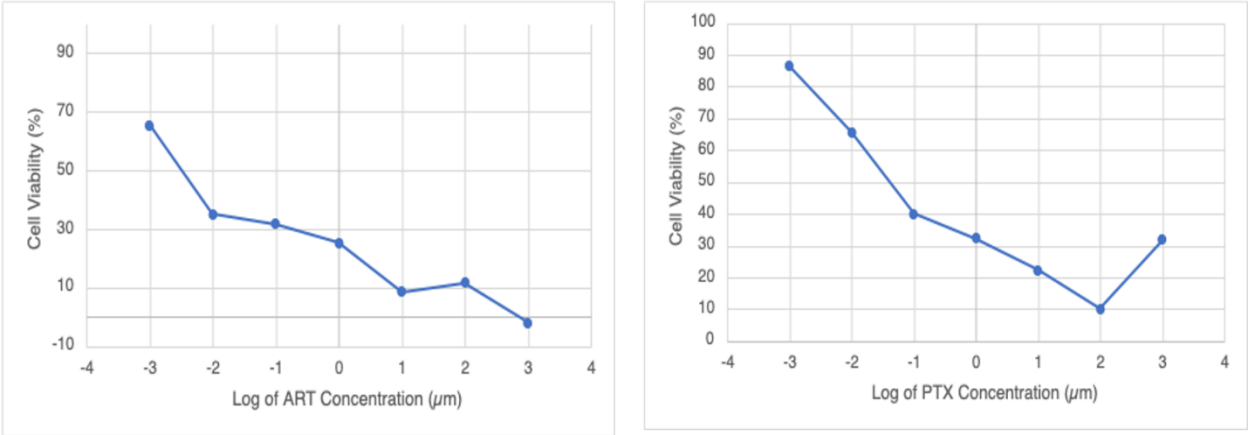

(A) (B)

Fig. 3: 72-hour MTT assay of cell viability of (A) ART and (B) PTX on LNCaP

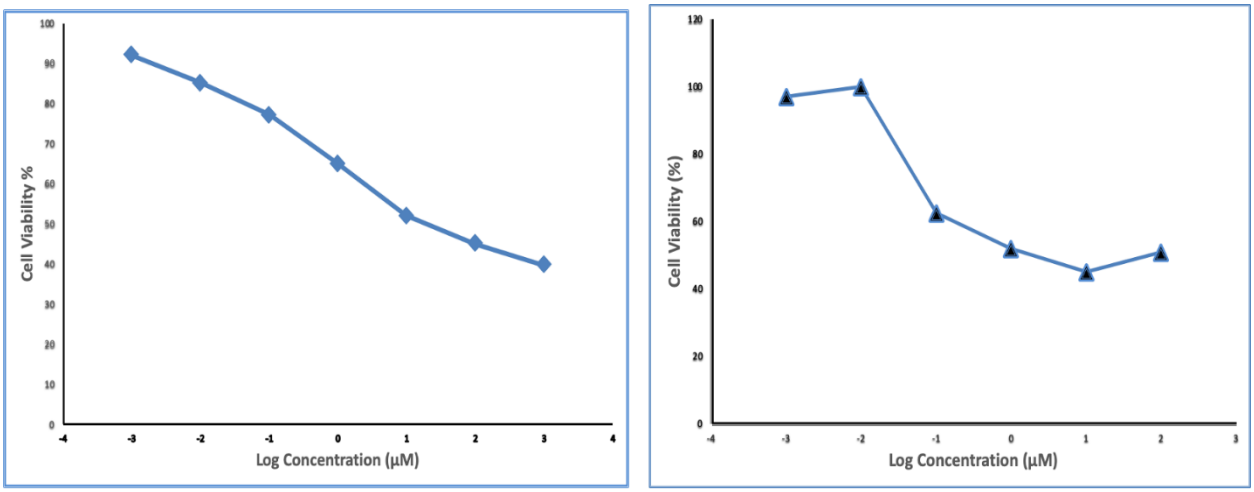

(A) (B)

Fig. 4: 120-hour MTS assay of cell viability of (A) ART and (B) PTX on PC-3

Cell Viability Study with Combination of ART+PTX

To evaluate whether ART improved chemosensitivity of PXT, both drugs were administered synergistically in different ratios and compared in PC-3 and LNCaP cell lines. The IC_{50} values of ART (25.1µM) and PTX 3.98(µM) in PC-3 cells, and ART (2.126µM) and PXT (0.05µM) in LNCaP cells using ratios 1:1, 1:2, 2:1. ART:PXT (2:1) ratio exhibited a greater inhibitory effect on cell viability (Fig 5.) than other ART:PXT combination ratios, ART and PTX solely in PC-3, 3 day treatment. ART:PXT (1:1) ratio exhibited a greater inhibitory effect on cell viability than other ART: PTX combination ratios, ART and PTX solely in LNCaP treatment 3-day treatment. These findings suggest that ART inhibits PCa cell proliferation and improves the chemosensitivity of PTX.

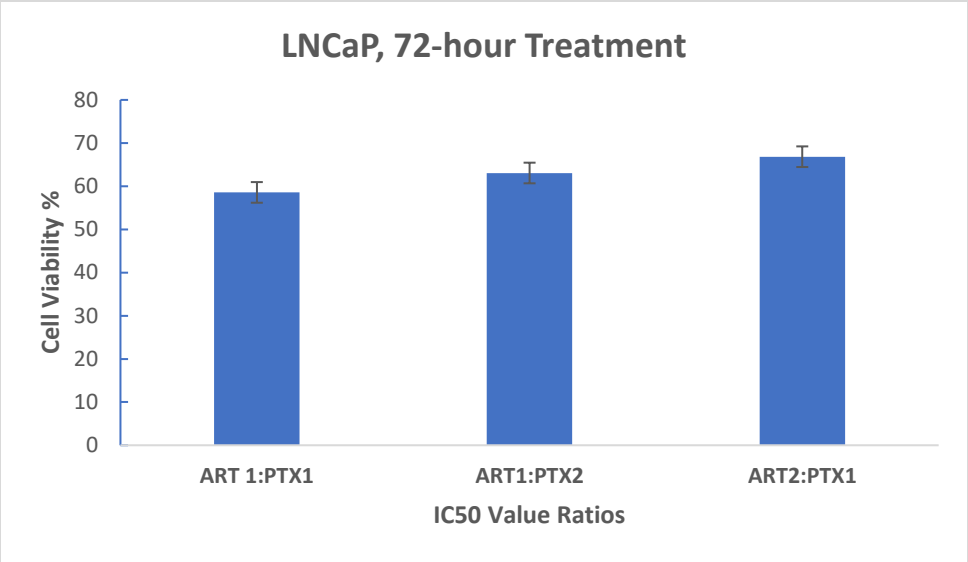

(A)

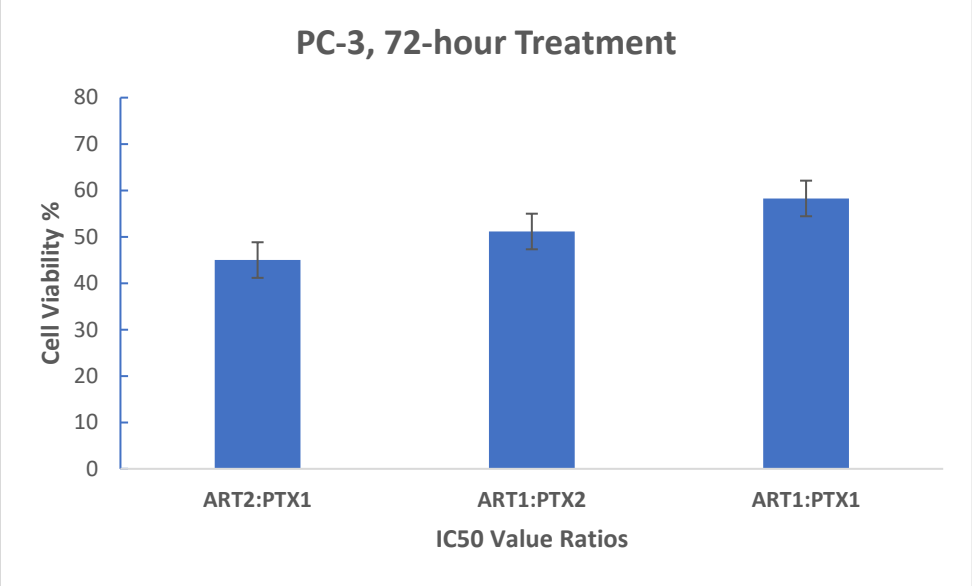

(B)

Fig. 5: Cell Viability Curve of ART + PXT ratios on cancer cell lines after 72 hours incubation on PCa. (A) LNCaP (B) PC-3

Apoptosis Activity Study with ART, PTX and ART+PTX

One of the earliest features of apoptosis is the translocation of phosphatidylserine from the inner to the outer leaflet of the plasma membrane, which can be detected by Annexin V. In late apoptosis and necrosis, it can be detected by a Propidium Iodide counter stain due to its ability to bind to DNA. This experiment assessed whether the augmentation of cell growth inhibition induced by ART in combination with PTX was associated with an increase in early and late apoptosis of PCa cells. The cells were treated with ART:PXT in PC-3 and LNCaP. After 72-hour and 120-hour of treatment, cells were labeled with Annexin V-fluorescein isothiocyanate/propidium iodide (PI) and analyzed by the Guava easyCyte single loader flow cytometry. The apoptotic effect on ART+PTX was determined to have an increase of early and late than in the single drug groups when examining both cell lines. As indicative there was a shift in population of cells towards the upper right quadrants that indicate early apoptosis moving towards a late stage of apoptosis in a time dependent manner from 3 to 5-day assays. In single ANOVA factory analysis, 72- and 120-hour annexin early apoptosis assay of PC-3 and LNCaP treated, P value was < 0.05. In a Tukey analysis, 72-hour annexin early apoptosis of PC-3 and LNCaP treated indicated a significant difference within treated groups and between untreated groups. In a Tukey analysis, 120-hour annexin early apoptosis of LNCaP there was not a significant difference between ART and PTX, but there was a significant difference between ART+PTX and all other treatments and control. In a Tukey analysis, 120-hour annexin early apoptosis of PC-3 there was not a significant difference between ART+PTX and ART, although there was a higher average in ART+PTX and ART. This suggests that ART combination with PTX significantly induces a significant degree of apoptosis in PCa cell lines.

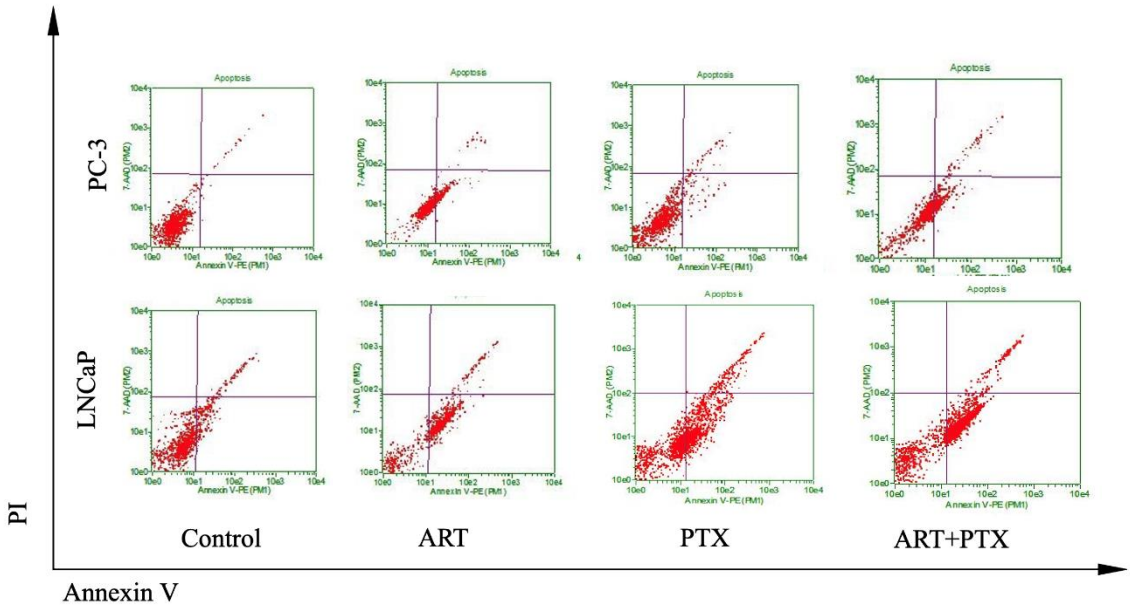
PC-3
LNCaP
PI
Control
ART
PTX
ART+PTX
Annexin V

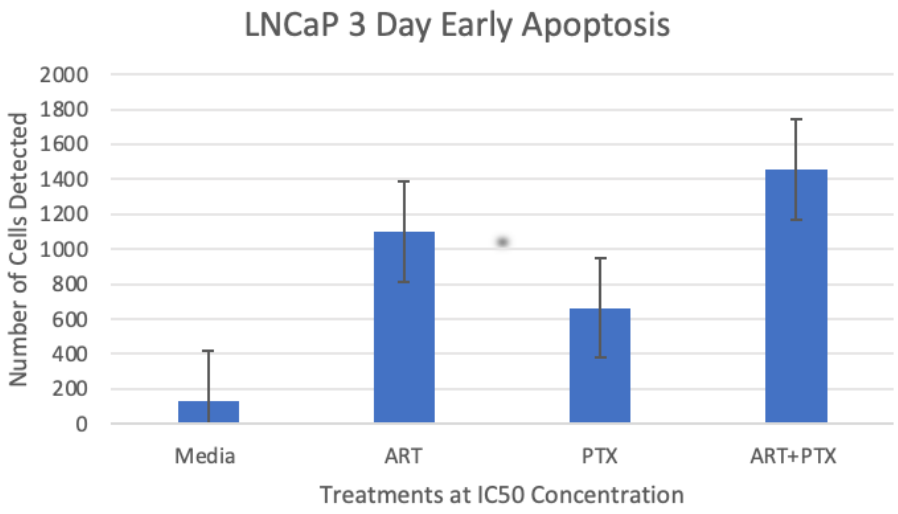
LNCaP 3 Day Early Apoptosis
Number of Cells Detected
2000
1800
1600
1400
1200
1000
800
600
400
200
0
Media
ART
PTX
ART+PTX
Treatments at IC50 Concentration

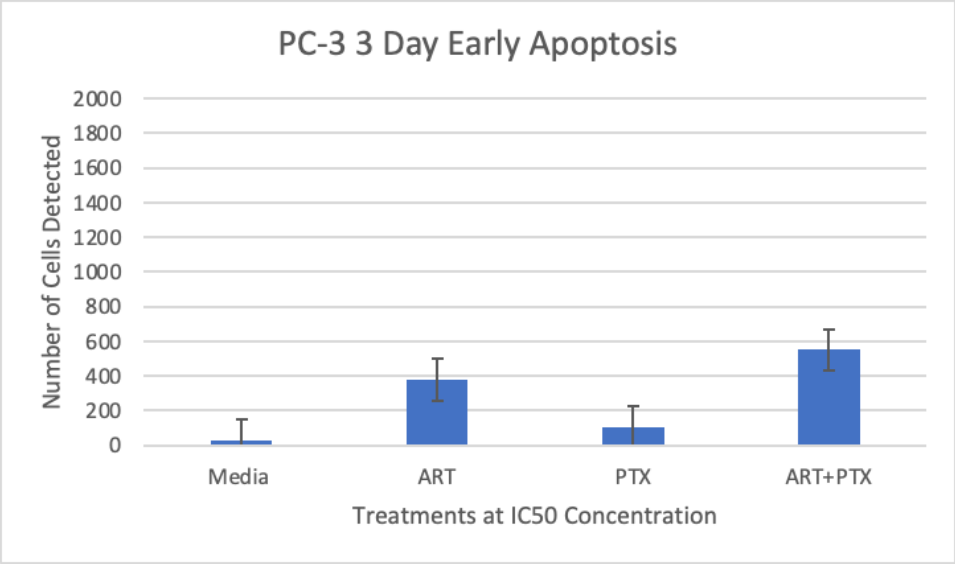

Fig. 6: Annexin V-FITC 3-day assay

Table 1. LNCaP 3 Day Early Apoptosis Single Factor ANOVA Analysis

ANOVA

Source of Variation	*SS*	*df*	*MS*	*F*	*P-value*	*F crit*
Between Groups	2946178.92	3	982059.639	180.509078	1.0989E-07	4.06618055
Within Groups	43524	8	5440.5			
Total	2989702.92	11				

Table 2. PC-3 3 Day Early Apoptosis Single Factor ANOVA Analysis

ANOVA

Source of Variation	*SS*	*df*	*MS*	*F*	*P-value*	*F crit*
Between Groups	4547446	3	1515815.33	1689.71519	1.516E-11	4.06618055
Within Groups	7176.66667	8	897.083333			
Total	4554622.67	11				

Table 3. LNCaP 3 Day Early Apoptosis Tukey Analysis

Tukey HSD Results

Treatments pair	Tukey HSD Q statistic	Tukey HSD p-value	Tukey HSD inferfence
MEDIA vs ART	22.7387	0.0010053	** p<0.01
Media vs PTX	12.5396	0.0010053	** p<0.01
Media vs ART+PTX	31.1532	0.0010053	** p<0.01
ART vs PTX	10.1992	0.0010053	** p<0.01
ART vs ART+PTX	8.4145	0.0015398	** p<0.01
PTX vs ART+PTX	18.6137	0.0010053	** p<0.01

Table 4. PC-3 3 Day Early Apoptosis Tukey Analysis

Tukey HSD Results

Treatments pair	Tukey HSD Q statistic	Tukey HSD p-value	Tukey HSD inferfence
MEDIA vs ART	41.1689	0.00101	** p<0.01
Media vs PTX	8.2416	0.00176	** p<0.01
Media vs ART+PTX	61.0666	0.00101	** p<0.01
ART vs PTX	32.9273	0.00101	** p<0.01
ART vs ART+PTX	19.8977	0.00101	** p<0.01
PTX vs ART+PTX	52.8249	0.00101	** p<0.01

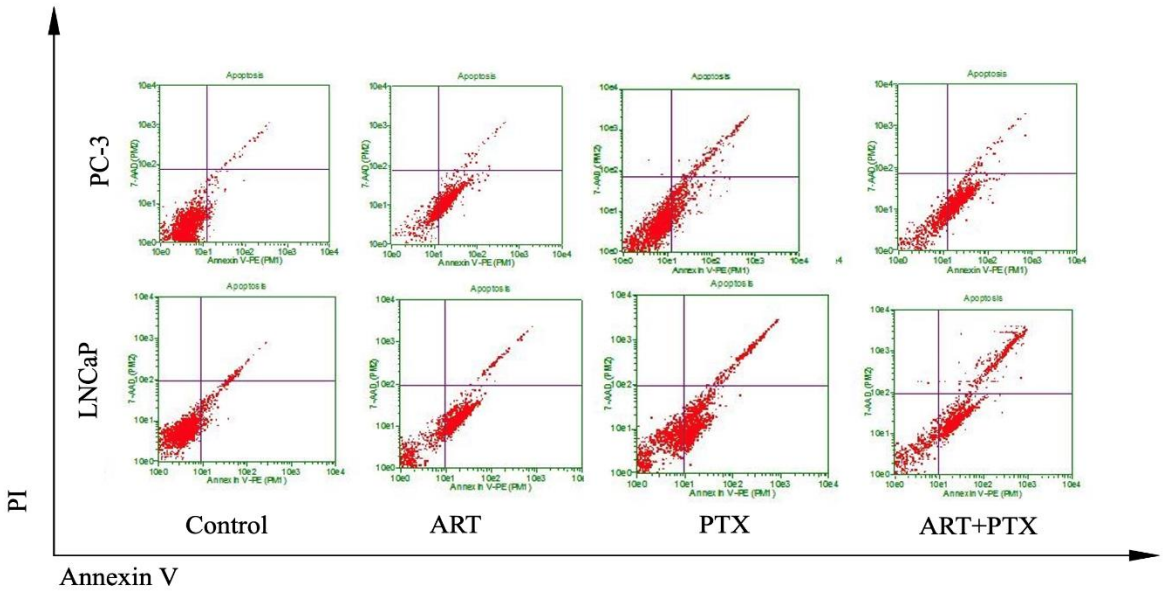
PC-3
LNCaP
PI
Control
ART
PTX
ART+PTX
Annexin V

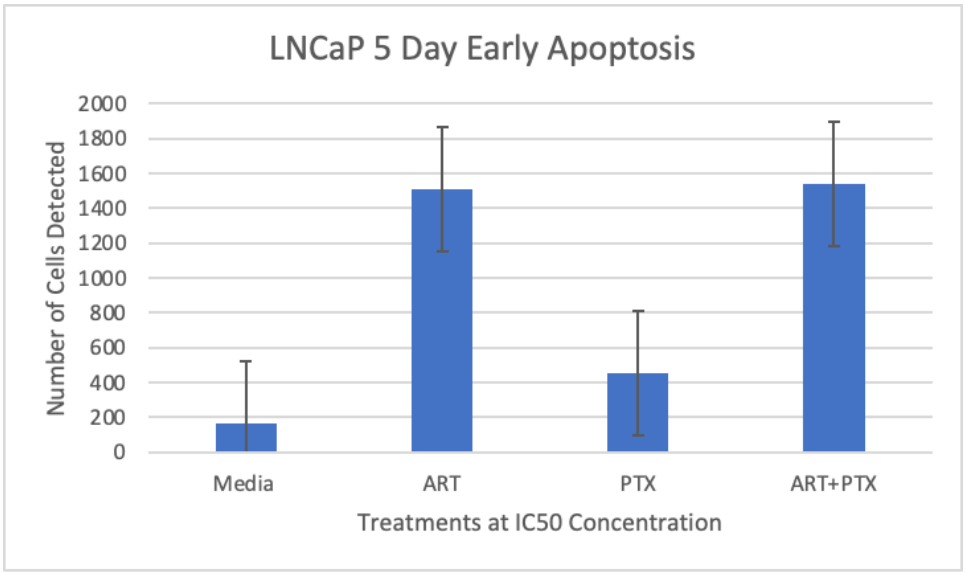
LNCaP 5 Day Early Apoptosis
Number of Cells Detected
2000
1800
1600
1400
1200
1000
800
600
400
200
0
Media
ART
PTX
ART+PTX
Treatments at IC50 Concentration

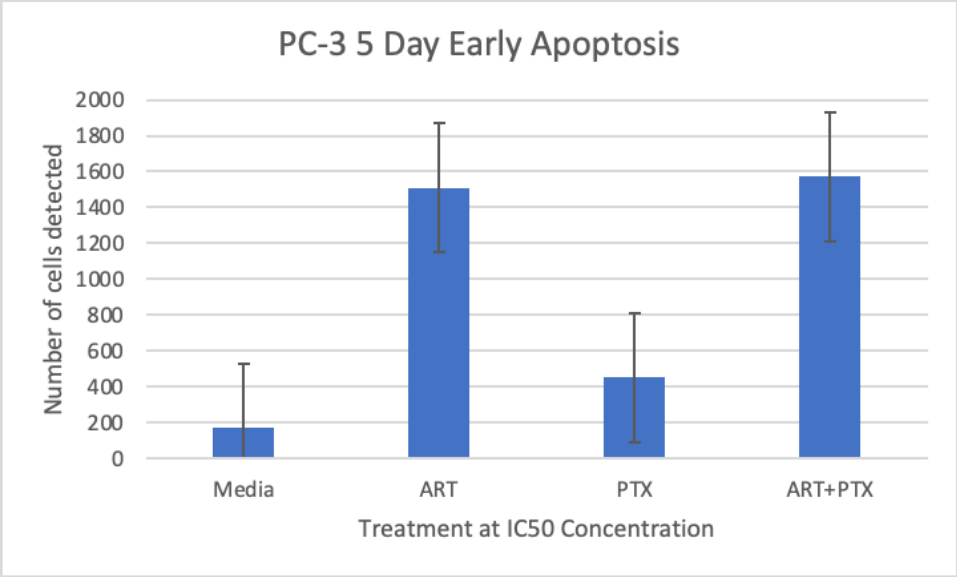

Fig. 7: Annexin V-FITC 5-day assay

Table 5. LNCaP 5 Day Early Apoptosis Single Factor ANOVA Analysis

ANOVA

Source of Variation	*SS*	*df*	*MS*	*F*	*P-value*	*F crit*
Between Groups	528193.583	3	176064.528	813.544218	2.8003E-10	4.06618055
Within Groups	1731.3333	8	216.41667			
Total	529924.917	11				

Table 6. PC-3 5 Day Early Apoptosis Single Factor ANOVA Analysis

ANOVA

Source of Variation	*SS*	*df*	*MS*	*F*	*P-value*	*F crit*
Between Groups	4674412.67	3	1558137.56	936.521446	1.5976E-10	4.06618055
Within Groups	13310	8	1663.75			
Total	4687722.67	11				

Table 7. LNCaP 5 Day Early Apoptosis Tukey Analysis

Tukey HSD Results

Treatments pair	Tukey HSD Q statistic	Tukey HSD p-value	Tukey HSD inferfence
MEDIA vs ART	22.4612	0.0010053	** p<0.01
Media vs PTX	18.5691	0.0010053	** p<0.01
Media vs ART+ PTX	27.1838	0.0010053	** p<0.01
ART vs PTX	3.892	0.0944272	insignificant
ART vs ART+PTX	4.7227	0.0412615	* p<0.05
PTX vs ART+PTX	8.6147	0.0013204	** p<0.01

Table 8. PC-3 3 Day Early Apoptosis Tukey Analysis

Tukey HSD Results

Treatments pair	Tukey HSD Q statistic	Tukey HSD p-value	Tukey HSD inferfence
MEDIA vs ART	56.9437	0.00101	** p<0.01
Media vs PTX	12.003	0.00101	** p<0.01
Media vs ART+PTX	59.633	0.00101	** p<0.01
ART vs PTX	44.9406	0.00101	** p<0.01
ART vs ART+PTX	2.6894	0.29957	insignificant
PTX vs ART+PTX	47.63	0.00101	** p<0.01

Subsequently, ART and PTX-induced growth inhibition in PCa cells was visualized by microscopy; the cells treated with ART and PTX for PC-3 and LNCaP cells. Cells cultured without these reagents exhibited characteristic normal growth and shape compared to cells treated with ART:PXT (Figure). In 120-hour for both controls exhibited over confluency. In addition, in a time-dependent increase of Annexin V fluorescence intensities accompanied by cell shrinkage in ART+PTX treated compared to ART and PXT solely when examined in PC-3 and LNCaP cells. Cell shrinkage was validated in a qualitative assessment when examined in inverted microscope imaging. This finding suggests that ART improved the chemosensitivity of PTX. MET in combination with PTX suppressed cell proliferation in a time-dependent manner.

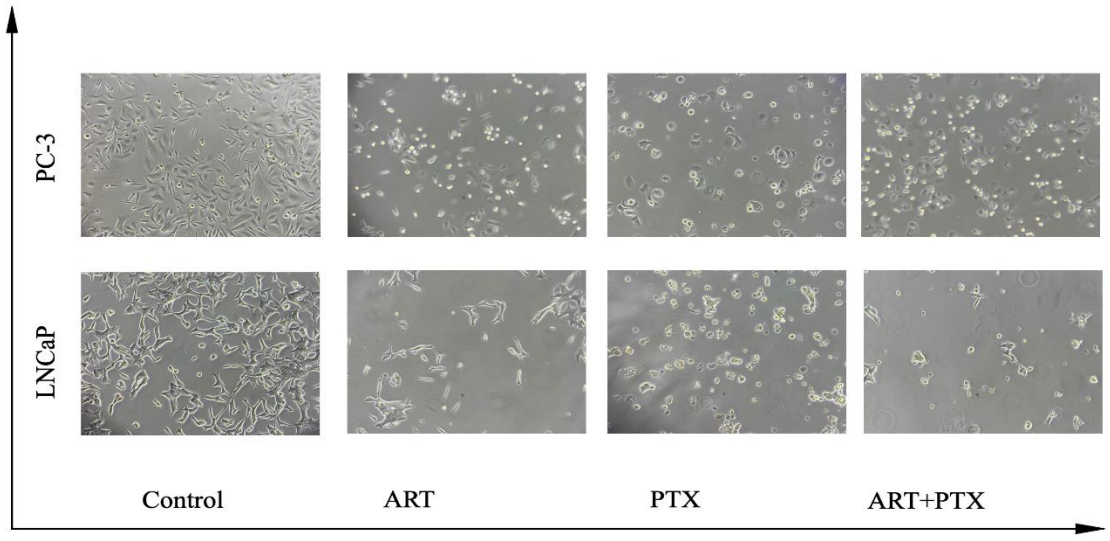

Fig. 8: Cell Morphology Examination in 72-hours

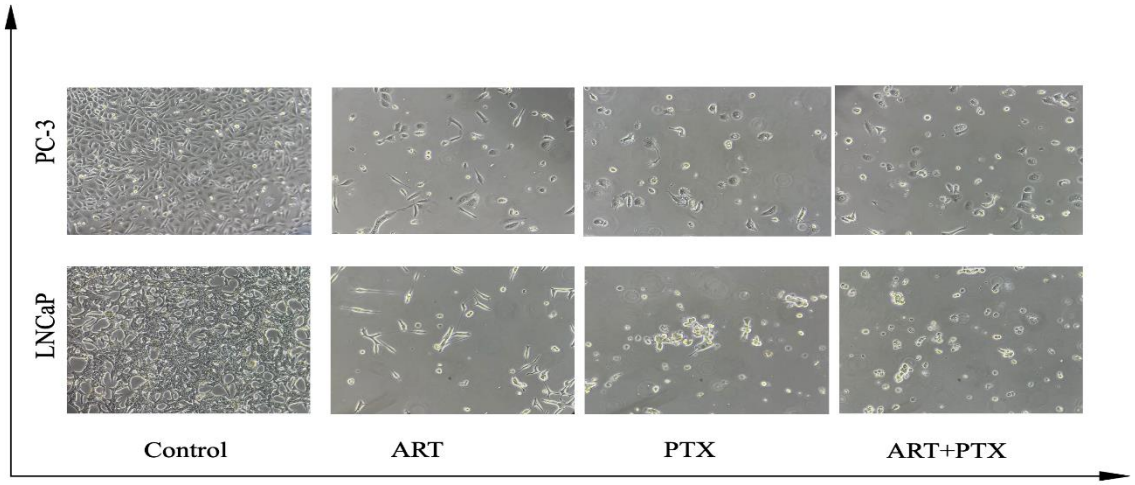

Fig. 9: Cell Morphology Examination in 120-hours

Caspase 3/7 Activity Study with ART, PTX and ART+PTX

A caspase-3/7 activity assay was used, as shown in Fig.10. The release of cytochrome c from mitochondria activates down- stream caspase molecules and lead to apoptotic cell death. To examine this, a flow cytometric caspase assay measured by examining the green, fluorescent intensities of caspase-3/7 activities of ART, PXT and ART+PTX treated on LNCaP cells at 72-hour time-point. As shown in Figure 10, caspase-3/7 activities were detected after 72 and 120-hours of ART+PTX exposure in LNCaP and PC-3. Results indicated there was higher caspase 3/7

activity in ART+PTX compared to control and other inducers in both cell lines at 72 and 120 hours. Triplicate trials in inducers and control had a P value <0.05 in all experiments. There is a right shift in population that probably indicates induction of caspase 3/7 protein. According to a Tukey test, control and inducers were significantly different from one another in PC-3 at 72-hours. In LNCaP, ART and PTX were not significantly different but ART+PTX were significantly different from ART, PTX, and control at 72 hours. In PC-3 at 120 hours, there is not a significant difference between ART+PTX and ART. In LNCaP, at 120 hours, ART and PTX were not significantly different but ART+PTX were significantly different from ART, PTX, and control.

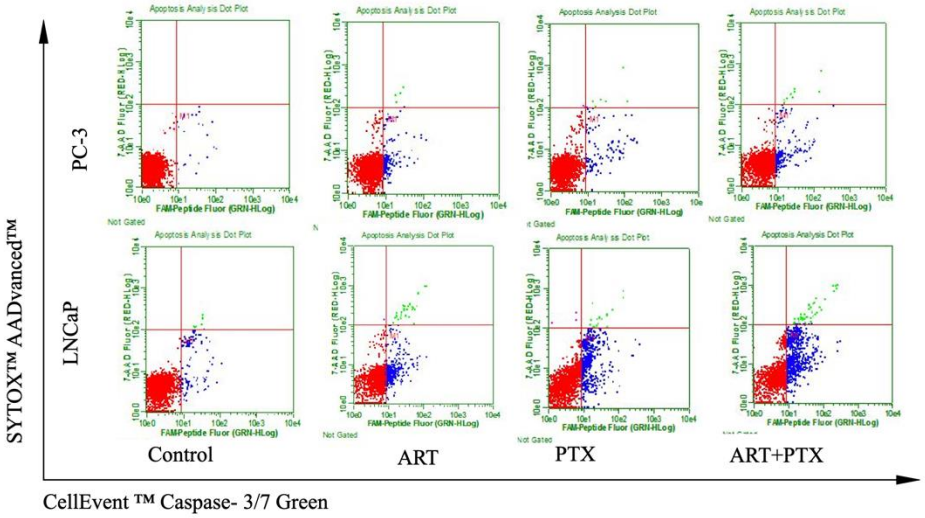

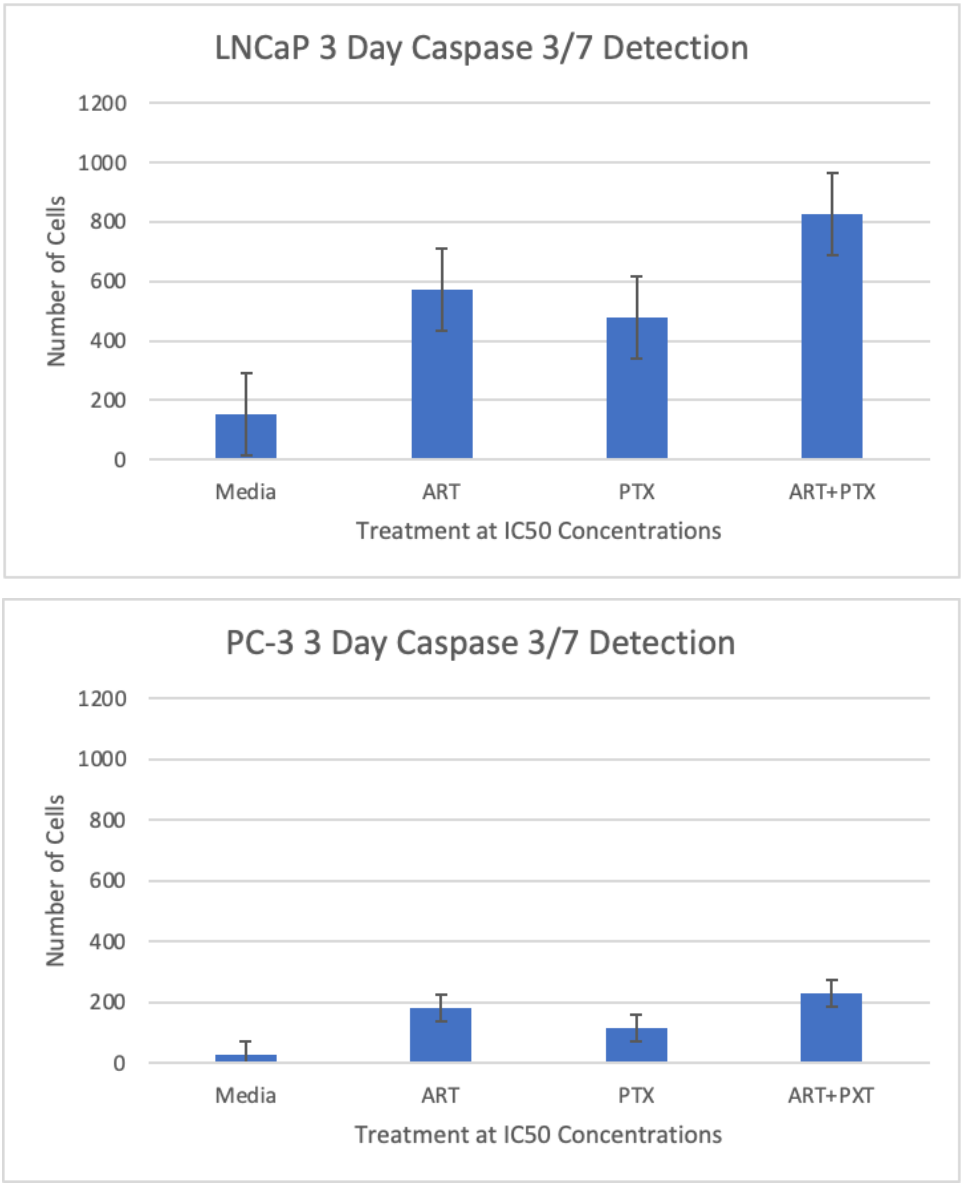

Fig. 10: Caspase 3/7, 3-day assay

Table 9. LNCaP 3 Day Caspase Single Factor ANOVA Analysis

ANOVA

Source of Variation	*SS*	*df*	*MS*	*F*	*P-value*	*F crit*
Between Groups	692127	3	230709	63.828745 3	6.2622E-06	4.0661805 5
Within Groups	28916	8	3614.5			
Total	721043	11				

Table 10. PC-3 3 Day Caspase Single Factor ANOVA Analysis

ANOVA

Source of Variation	*SS*	*df*	*MS*	*F*	*P-value*	*F crit*
Between Groups	69934.25	3	23311.4167	77.812795	2.9268E-06	4.0661805
Within Groups	2396.66667	8	299.58333			
Total	72330.9167	11				

Table 11. LNCaP 3 Day Caspase 3/7 Detection Tukey Analysis

Tukey HSD Results

Treatments pair	Tukey HSD Q statistic	Tukey HSD p-value	Tukey HSD inferfence
MEDIA vs ART	12.0136	0.0010053	** p<0.01
Media vs PTX	9.3151	0.0010053	** p<0.01
Media vs ART+ PTX	19.3312	0.0010053	** p<0.01
ART vs PTX	2.6985	0.2971356	insignificant
ART vs ART+PTX	7.3176	0.0037486	** p<0.01
PTX vs ART+PTX	10.0161	0.0010053	** p<0.01

Table 12. PC-3 3 Day Caspase 3/7 Detection Tukey Analysis

Tukey HSD Results

Treatments pair	Tukey HSD Q statistic	Tukey HSD p-value	Tukey HSD inferfence
MEDIA vs ART	15.4774	0.0010053	** p<0.01
Media vs PTX	8.8728	0.0010843	** p<0.01
Media vs ART+ PTX	20.3808	0.0010053	** p<0.01
ART vs PTX	6.6046	0.0069615	** p<0.01
ART vs ART+PTX	4.9034	0.0345246	* p<0.05
PTX vs ART+PTX	11.508	0.0010053	** p<0.01

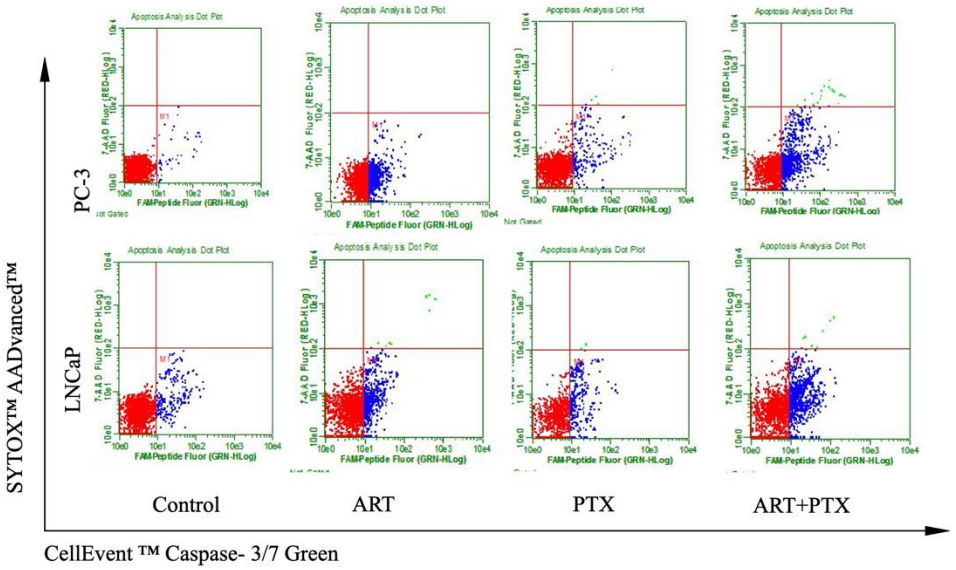
PC-3
LNCaP
SYTOX™ AADvanced™
Control
ART
PTX
ART+PTX
CellEvent ™ Caspase- 3/7 Green

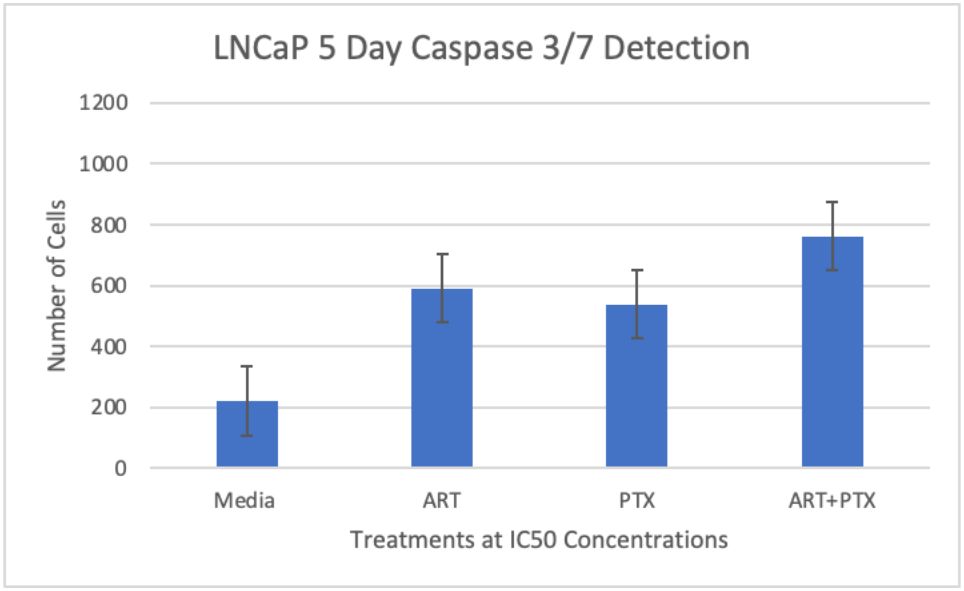
LNCaP 5 Day Caspase 3/7 Detection
Number of Cells
1200
1000
800
600
400
200
0
Media
ART
PTX
ART+PTX
Treatments at IC50 Concentrations

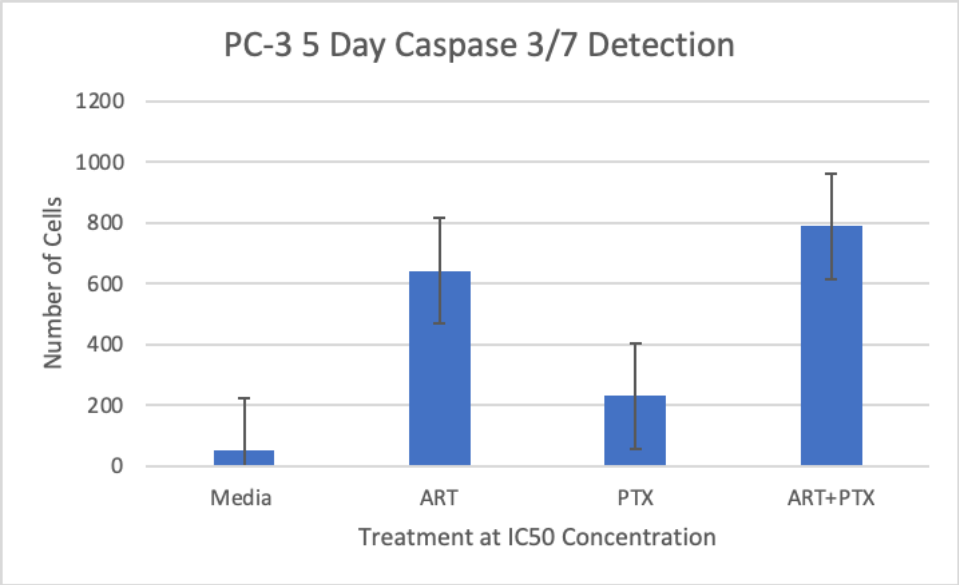

Fig. 11: Caspase 3/7, 5-day assay

Table 13. LNCaP 5 Day Caspase Single Factor ANOVA Analysis

ANOVA

Source of Variation	*SS*	*df*	*MS*	*F*	*P-value*	*F crit*
Between Groups	460451	3	153483.667	113.306921	6.8156E-07	4.06618055
Within Groups	10836.6667	8	1354.58333			
Total	471287.667	11				

Table 14. PC-3 5 Day Caspase Single Factor ANOVA Analysis

ANOVA

Source of Variation	*SS*	*df*	*MS*	*F*	*P-value*	*F crit*
Between Groups	1071333.67	3	357111.222	56.3985979	1.0038E-05	4.06618055
Within Groups	50655.3333	8	6331.91667			
Total	1121989	11				

Table 15. LNCaP 5 Day Caspase 3/7 Detection Tukey Analysis

Tukey HSD Results

Treatments pair	Tukey HSD Q statistic	Tukey HSD p-value	Tukey HSD inferfence
MEDIA vs ART	17.4438	0.0010053	** p<0.01
Media vs PTX	14.9496	0.0010053	** p<0.01
Media vs ART+ PTX	25.4912	0.0010053	** p<0.01
ART vs PTX	2.4942	0.355484	insignificant
ART vs ART+PTX	8.0474	0.0020561	** p<0.01
PTX vs ART+PTX	10.5416	0.0010053	** p<0.01

Table 16. PC-3 5 Day Caspase 3/7 Detection Tukey Analysis

Tukey HSD Results

Treatments pair	Tukey HSD Q statistic	Tukey HSD p-value	Tukey HSD inferfence
MEDIA vs ART	12.8859	0.0010053	** p<0.01
Media vs PTX	3.9253	0.0913423	insignificant
Media vs ART+ PTX	16.0566	0.0010053	** p<0.01
ART vs PTX	8.9606	0.001014	** p<0.01
ART vs ART+PTX	3.1707	0.1916508	insignificant
PTX vs ART+PTX	12.1313	0.0010053	** p<0.01

ROS Activity Study with ART, PTX and ART+PTX

ROS forms as a natural byproduct of the normal metabolism of oxygen. However, ROS level can increase dramatically upon environmental or chemical stress (e.g., presence of cytotoxic agent). To examine whether exposure of ART promotes ROS intracellular production, LNCaP cells were stained live cells with DCFH-DA dye, 72-hours after ART, PXT, ART+PXT treatment. In addition, PC-3 cell lines were stained with DCFH-DA dye, 120-hours after ART, PXT, ART+ PXT treatment. DCFH-DA is rapidly oxidized to DCF by ROS and the fluorescent intensities were measured with the Guava easyCyte Single loader flow cytometer. As shown in Figure 12, the levels of DCF fluorescence in PC-3 cells treated with ART+PXT were significantly increased in a

dose-dependent manner. The levels of DCF fluorescence in LNCaP when treated with ART+PXT was relatively the same when treated with ART solely. The imbalance of ROS may promote mitochondrial dysfunction and lead to mitochondria-mediated apoptosis due to the presence of ART as supported by literature.

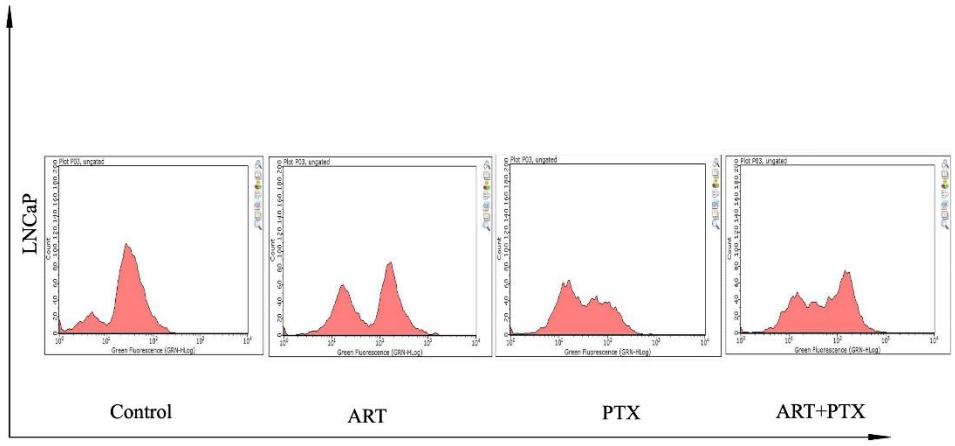

Fig. 12: LNCaP 72-hour ROS activity assay

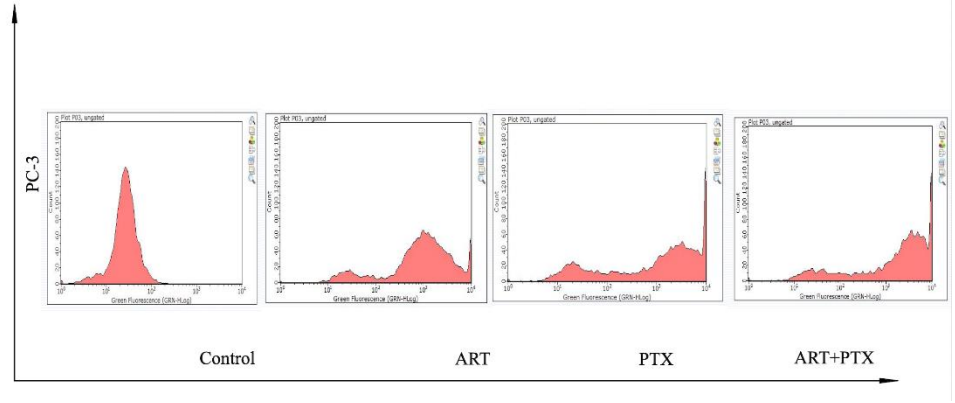

Fig. 13: PC-3 120-hour ROS activity assay

CHAPTER V

DISCUSSION

Prostate cancer is one of the most common causes of cancer related death worldwide in men. The failure of prostate cancer treatment with paclitaxel occurs mostly due to the development of resistance to the drug. Averting the phenomenon of paclitaxel resistance development could be a very promising method for successful chemotherapy and eradication of prostate cancer. Recently, several studies have shown that the induction of ROS dependent apoptosis is a potential target for cancer therapy and the induction of apoptosis in response to therapeutics can be viewed as having a pro-death or pro-survival role, which contributes to the anticancer efficacy of these drugs as well as drug resistance. Many studies have reported that ART induces apoptosis via ROS activity, this could increase the potency of various anticancer drugs such as paclitaxel. However, there are no reports of averting the phenomenon of drug resistance development by the modulating apoptosis with Artesunate, thus in this study explored whether apoptosis induction of Artesunate could avert the development of resistance against paclitaxel in prostate cancer cell lines.

The study demonstrated that pre-treatment of PC-3 cells with ART and PXT had IC50 values of 25.1 and 3.96 at 120 hours and LNCaP treatment with ART and PXT had IC50 values of 2.142 and 0.05 at 72 hours. LNCaP has higher sensitivity to ART and PXT than PC-3. This can speculate that drugs may sensitize AR dependence prostate cancer to induce cell death at a faster rate. Prostate cancer cells were treated with different ratios of ART+PXT in a 72-hour dependent manner. In PC-3 cell line, ART:PXT (2:1) had the highest cytotoxicity compared to other ratios and PXT and ART solely. In LNCaP cell line, ART:PXT (1:1) had the highest cytotoxicity compared to other ratios and PXT and ART solely. This validates that ART+ PXT has a greater cytotoxic effect than ART and PXT solely.

Early and late apoptosis was detected in an Annexin-PI FITC. It was observed that when PC-3 cells were treated with PXT solely in a 72 and 120 –hour there was a substantial number of viable cells in comparison to ART and ART+PTX. The treatment of ART and ART+ PTX indicated a shift in the population of cells towards early and mid-apoptosis. ART+PTX had the highest degree of apoptotic cells as seen in figures 6 and 7. In LNCaP 72 and 120-hour had a higher sensitivity to PTX, this indicated by the shift of population compared to PC-3 samples. ART + PTX had the highest degree of apoptotic cells as seen in figure 6 and 7. Late apoptosis was observed in both cell lines, it can be speculated it is due to the time dependent manner in which the assays were carried out. These claims can be validated by microscopy examination of cells before apoptotic assay analysis. The inverted microscope images revealed pseudopodal shrinkage and cell turned round following the treatment of ART, PTX, and ART+PTX indicating apoptosis compared to control in both prostate cancer cell lines. Cell shrinkage is a common indicator of apoptosis. Although ART demonstrated clusters formation such as of those of viable cells there is cell shrinkage. In a time dependent manner there was more cell shrinkage and less cell adherence in ART+PTX 120-hour compared to ART+PTX 72-hour. ART+ PXT in both cell lines were also compared to control that demonstrated full confluent cells which clustered and exhibited normal physiological. This validates there is induction of apoptosis by ART, PTX, ART+PTX, and is further supported by Annexin PI FITC assay that ART+ PTX has a higher degree of apoptosis than ART and PTX solely.

Caspase activity was examined using CellEvent Caspase 3/7 activity assay. As shown in Figure 10, significant in caspase-3/7 activities were detected after 72 and 120 hours of control, ART, PTX, and ART+PTX exposure in PC-3 and LNCaP. There is a shift of viable population in all induced samples compared to control. This is an indicator of induction of apoptosis by caspases.

Results indicated there was higher caspase 3/7 activity in ART+PTX compared to control and other inducers in both cell lines at 72 and 120 hours. Triplet trials in inducers and control had a P value <0.05 in all experimental sessions. According to a Tukey test, control and inducers

were significantly different from one another in PC-3 at 72-hours. In LNCaP, at 72 and 120 hours, ART and PTX were not significantly different but ART+PTX were significantly different from ART, PTX, and control. In PC-3 at 120 hours, there is not a significant difference between ART+PTX and ART. There is a trend in PC-3 at 120-hour exposure that reveals there is not a significant difference between ART+PTX and ART in both caspase and apoptosis assay.

ROS activity was measured using DCFDA to assess the intensity of reactive oxygen species produced by ART, PTX and ART+PTX. All inducers produced low to high ROS activity compared to control in both PC-3 and LNCaP. In PC-3 cancer cell lines, ART+PTX had the highest ROS activity indicated by a shift of intensity towards high ROS activity compared to ART and PTX. This can speculate that apoptosis may be induced via ROS activity. When examining LNCaP cells at 72-hour there was not a significant difference between ART+PTX and ART, although both were higher than PTX indicating ROS activity is low when treated with PTX. LNCaP cancer cell lines may need to be assessed at 120-hour to fully elucidate whether ART+ PTX has a higher ROS activity than ART and PTX solely.

These findings support the idea that ART +PTX induces a higher degree of apoptosis, ROS activity, caspase activity than ART and PTX solely on LNCaP and PC-3. This study could provide a strategy to prevent the development of taxol resistance with time in prostate cancer cell lines. Artesunate with paclitaxel can aid in paclitaxel resistant prostate cancer towards taxol and reduce its metastatic potential by causing ROS triggered, caspase-mediated cellular apoptosis in prostate cancer. These findings provide promising insights into a novel, potential therapeutic strategies for Pca.

Future work includes detection of protein expression levels of proapoptotic and antiapoptotic protein such as Bax, Bcl-2, Bcl-xL, in response to ART, PXT and ART+PTX using western blot. Protein expression can further validate if ART+PTX potentiates apoptosis via ROS. Combination studies should be performed on normal cell lines to validate its cytotoxic effects target prostate cancer cells in comparison to those of normal cells. Additional caspase 3/7 activity of ART+PTX on PC-3 in 72 and 120-hour and 120-hour in LNCaP to elucidate

mechanism of ART+PTX. Further studies on cell cycle arrest at G2/M need to be conducted to validate that artesunate can potentiate paclitaxel resistance and mechanism of action.

REFERENCES

1. Arbab, I. A., Looi, C. Y., Abdul, A. B., Cheah, F. K., Wong, W. F., Sukari, M. A., ... & Ibrahim Abdelwahab, S. (2012). Dentatin induces apoptosis in prostate cancer cells via Bcl-2, Bcl-xL, Survivin downregulation, caspase-9,-3/7 activation, and NF-κB inhibition. *Evidence-Based Complementary and Alternative Medicine*, *2012*.
2. Archer M, Dogra N, Kyprianou N. Inflammation as a Driver of Prostate Cancer Metastasis and Therapeutic Resistance. *Cancers*. 2020; 12(10):2984. https://doi.org/10.3390/cancers12102984
3. Baker, A. M., Oberley, L. W., & Cohen, M. B. (1997). Expression of antioxidant enzymes in human prostatic adenocarcinoma. *The Prostate*, *32*(4), 229–233. https://doi.org/10.1002/(sici)1097-0045(19970901)32:4<229::aid-pros1>3.0.co;2-e
4. Balaji, N et al. "Annexin v - affinity assay - apoptosis detection system in granular cell ameloblastoma." *Journal of international oral health : JIOH* vol. 5,6 (2013): 25-30.
5. Bumbaca, B., & Li, W. (2018). Taxane resistance in castration-resistant prostate cancer: mechanisms and therapeutic strategies. *Acta pharmaceutica Sinica. B*, *8*(4), 518–529. https://doi.org/10.1016/j.apsb.2018.04.007
6. Crespo-Ortiz, M. P., & Wei, M. Q. (2012). Antitumor activity of artemisinin and its derivatives: from a well-known antimalarial agent to a potential anticancer drug. *Journal of biomedicine & biotechnology*, *2012*, 247597. https://doi.org/10.1155/2012/247597
7. Datta, S., Choudhury, D., Das, A. *et al.* Autophagy inhibition with chloroquine reverts paclitaxel resistance and attenuates metastatic potential in human nonsmall lung adenocarcinoma A549 cells via ROS mediated modulation of β-catenin pathway. *Apoptosis* **24,** 414–433 (2019). https://doi.org/10.1007/s10495-019-01526-y
8. Di Zazzo, Galasso, Giovannelli, Di Donato, Bilancio, Perillo, Sinisi, Migliaccio, & Castoria. (2019). Estrogen Receptors in Epithelial-Mesenchymal Transition of Prostate Cancer. *Cancers*, *11*(10), 1418. https://doi.org/10.3390/cancers11101418
9. Dozmorov, M. G., Hurst, R. E., Culkin, D. J., Kropp, B. P., Frank, M. B., Osban, J., Penning, T. M., & Lin, H. K. (2009). Unique patterns of molecular profiling between human prostate cancer LNCaP and PC-3 cells. *The Prostate*, *69*(10), 1077–1090. https://doi.org/10.1002/pros.20960
10. Greenshields, A. L., Fernando, W., & Hoskin, D. W. (2019). The anti-malarial drug artesunate causes cell cycle arrest and apoptosis of triple-negative MDA-MB-468 and HER2-enriched SK-BR-3 breast cancer cells. *Experimental and molecular pathology*, *107*, 10-22.
11. Greenshields, A. L., Shepherd, T. G., & Hoskin, D. W. (2017). Contribution of reactive oxygen species to ovarian cancer cell growth arrest and killing by the anti-malarial drug artesunate. *Molecular carcinogenesis*, *56*(1), 75-93.
12. Greten, F. R., & Grivennikov, S. I. (2019). Inflammation and Cancer: Triggers, Mechanisms, and Consequences. *Immunity*, *51*(1), 27–41. https://doi.org/10.1016/j.immuni.2019.06.025

13. Habib A, Jaffar G, Khalid MSZ, Hussain Z, Zainab SW, Ashraf Z, Haroon A, Javed R, Khalid B, Habib P, Risk Factors Associated with Prostate Cancer, Journal of Drug Delivery and Therapeutics. 2021; 11(2):188-193 DOI: **http://dx.doi.org/10.22270/jddt.v11i2.4758**
14. He, L., Fang, H., Chen, C., Wu, Y., Wang, Y., Ge, H., Wang, L., Wan, Y., & He, H. (2020). Metastatic castration-resistant prostate cancer: Academic insights and perspectives through bibliometric analysis. *Medicine*, *99*(15), e19760. https://doi.org/10.1097/MD.0000000000019760
15. Hinton, B., Adedeji, D. and Payne, G. (2017) *In-Vitro* Antiproliferative Analysis of Metformin Hydrochloride on Androgen-Sensitive, LNCAP and Androgen-Insensitive, PC-3 Human Prostate Cancer Cell Lines. *Pharmacology & Pharmacy*, **8**, 85-89. doi: 10.4236/pp.2017.83006.
16. Iang, H., Zhang, X. W., Liao, Q. L., Wu, W. T., Liu, Y. L., & Huang, W. H. (2019). Electrochemical Monitoring of Paclitaxel-Induced ROS Release from Mitochondria inside Single Cells. *Small (Weinheim an der Bergstrasse, Germany)*, *15*(48), e1901787. https://doi.org/10.1002/smll.201901787
17. Kim, H., & Xue, X. (2020). Detection of Total Reactive Oxygen Species in Adherent Cells by 2',7'-Dichlorodihydrofluorescein Diacetate Staining. *Journal of visualized experiments : JoVE*, (160), 10.3791/60682. https://doi.org/10.3791/60682
18. Lai, X., Li, Q., Wu, F., Lin, J., Chen, J., Zheng, H., & Guo, L. (2020). Epithelial-Mesenchymal Transition and Metabolic Switching in Cancer: Lessons From Somatic Cell Reprogramming. *Frontiers in cell and developmental biology*, *8*, 760. https://doi.org/10.3389/fcell.2020.00760
19. Leslie, S. W., Soon-Sutton, T. L., Sajjad, H., et al. (2021). Prostate cancer. [Updated 2021 Sep 17]. In: *StatPearls*[Internet]. Retrieved on Oct. 31, 2021 from https://www.ncbi.nlm.nih.gov/books/NBK470550/
20. Li Z, Li Q, Wu J, Wang M, Yu J. Artemisinin and Its Derivatives as a Repurposing Anticancer Agent: What Else Do We Need to Do? Molecules. 2016 Oct 7;21(10):1331. doi: 10.3390/molecules21101331. PMID: 27739410; PMCID: PMC6272993.
21. Ma Z, Woon CY, Liu CG, et al. Repurposing Artemisinin and its Derivatives as Anticancer Drugs: A Chance or Challenge? Frontiers in Pharmacology. 2021 ;12:828856. DOI: 10.3389/fphar.2021.828856
22. Mahmood, T., & Yang, P. C. (2012). Western blot: technique, theory, and trouble shooting. *North American journal of medical sciences*, *4*(9), 429–434. https://doi.org/10.4103/1947-2714.100998
23. Pang, Y., Qin, G., Wu, L., Wang, X., & Chen, T. (2016). Artesunate induces ROS-dependent apoptosis via a Bax-mediated intrinsic pathway in Huh-7 and Hep3B cells. *Experimental cell research*, *347*(2), 251–260. https://doi.org/10.1016/j.yexcr.2016.06.012
24. Ren, X., Zhao, B., Chang, H., Xiao, M., Wu, Y., & Liu, Y. (2018). Paclitaxel suppresses proliferation and induces apoptosis through regulation of ROS and the AKT/MAPK signaling pathway in canine mammary gland tumor cells. Molecular Medicine Reports, 17, 8289-8299. https://doi.org/10.3892/mmr.2018.8868
25. Saleh, S. A., Adly, H. M., Abdelkhaliq, A. A., & Nassir, A. M. (2020). Serum levels of selenium, zinc, copper, manganese, and iron in prostate cancer patients. *Current urology*, *14*(1), 44-49.

26. Shen, Y., Zhang, B., Su, Y., Badshah, S. A., Wang, X., Li, X., ... & Shang, P. (2020). Iron promotes dihydroartemisinin cytotoxicity via ROS production and blockade of autophagic flux via lysosomal damage in osteosarcoma. *Frontiers in Pharmacology*, *11*, 444.
27. Surveillance, Epidemiology, and End Results Program (SEER 2019). National Cancer Institute, NIH. Retrieved 12 October 2019.
28. Tai, S., Sun, Y., Squires, J. M., Zhang, H., Oh, W. K., Liang, C. Z., & Huang, J. (2011). PC3 is a cell line characteristic of prostatic small cell carcinoma. *The Prostate*, *71*(15), 1668–1679. https://doi.org/10.1002/pros.21383
29. Teo, M. Y., Rathkopf, D. E., & Kantoff, P. (2019). Treatment of Advanced Prostate Cancer. *Annual review of medicine*, *70*, 479–499. https://doi.org/10.1146/annurev-med-051517-011947
30. Wadosky, K. M., & Koochekpour, S. (2016). Molecular mechanisms underlying resistance to androgen deprivation therapy in prostate cancer. *Oncotarget*, *7*(39), 64447–64470. https://doi.org/10.18632/oncotarget.10901
31. Wang, X., An, P., Zeng, J., Liu, X., Wang, B., Fang, X., ... & Min, J. (2017). Serum ferritin in combination with prostate-specific antigen improves predictive accuracy for prostate cancer. *Oncotarget*, *8*(11), 17862.
32. Yang, N. D., Tan, S. H., Ng, S., Shi, Y., Zhou, J., Tan, K. S. W., ... & Shen, H. M. (2014). Artesunate induces cell death in human cancer cells via enhancing lysosomal function and lysosomal degradation of ferritin. *Journal of Biological Chemistry*, *289*(48), 33425-33441.
33. Yang, X., Zheng, Y., Liu, L., Huang, J., Wang, F., & Zhang, J. (2021). Progress on the study of the anticancer effects of artesunate (Review). Oncology Letters, 22, 750. https://doi.org/10.3892/ol.2021.13011
34. Yin, S., Yang, H., Zhao, X., Wei, S., Tao, Y., Liu, M., Bo, R., & Li, J. (2020). Antimalarial agent artesunate induces G0/G1 cell cycle arrest and apoptosis via increasing intracellular ROS levels in normal liver cells. *Human & Experimental Toxicology*, 1681–1689. https://doi.org/10.1177/0960327120937331
35. Yu, P., Duan, X., Cheng, Y., Liu, C., Chen, Y., Liu, W., Yin, B., Wang, X., & Tao, Z. (2017). Androgen-independent LNCaP cells are a subline of LNCaP cells with a more aggressive phenotype and androgen suppresses their growth by inducing cell cycle arrest at the G1 phase. *International journal of molecular medicine*, *40*(5), 1426–1434. https://doi.org/10.3892/ijmm.2017.3125
36. Zhang, X. Interactions between cancer cells and bone microenvironment promote bone metastasis in prostate cancer. *Cancer Commun* 39, 76 (2019). https://doi.org/10.1186/s40880-019-0425-1
37. Zhao, Y., Jiang, W., Li, B., Yao, Q., Dong, J., Cen, Y., ... & Zhou, H. (2011). Artesunate enhances radiosensitivity of human non-small cell lung cancer A549 cells via increasing NO production to induce cell cycle arrest at G2/M phase. *International immunopharmacology*, *11*(12), 2039-2046.
38. Zhao, Y., Zeng, X., Tang, H., Ye, D., & Liu, J. (2019). Combination of metformin and paclitaxel suppresses proliferation and induces apoptosis of human prostate cancer cells via oxidative stress and targeting the mitochondria dependent pathway. Oncology Letters, 17, 4277-4284. https://doi.org/10.3892/ol.2019.10119